

## Time domain identification, frequency domain identification. Equivalencies! Differences?

J. Schoukens, R. Pintelon, and Y. Rolain  
 Vrije Universiteit Brussel, Department ELEC, Pleinlaan 2, B1050 Brussels, Belgium  
 email: johan.schoukens@vub.ac.be

**Abstract** - In the first part of this paper, the full equivalence between time and frequency domain identification is established. Next the differences that show up in the practical applications are discussed. Finally, an illustration on the identification of a servo-system in feedback is given.

### I. INTRODUCTION

For a long time, frequency domain identification and time domain identification were considered as competing methods to solve the same problem: building a model for a linear time-invariant dynamic system. In the end, the frequency domain approach got a bad reputation because the transformation of the data from the time domain to the frequency domain is prone to leakage errors: noiseless data in the time domain resulted in noisy frequency response function (FRF) measurements. This is illustrated in the simulation below. A system is excited with a random input. The input  $u_0(t)$  and the output  $y_0(t)$  are sampled in 256 points  $u_0(k), y_0(k)$  with  $k = 1, 2, \dots, 256$ . No disturbing noise is added. Starting from these measurements, the FRF  $\hat{G}(j\omega_c)$  is measured and compared to the true FRF  $G_0$  (FIG. 1.). It can be seen that  $\hat{G}$  is strongly disturbed. This was the major reason to drop the frequency domain approach. The statement: Why would we move from the time to the frequency domain? The only thing we buy for it are problems! expresses very well the feeling that lived in the identification society.

This problem is further analysed in Section III where it is shown that i) exactly the same problem is present in the time domain; ii) by extending the models, a full equivalence exists between both domains.

Once this equivalence between both domains is established, one can wonder why to bother about it? Are there any differences at all? The answer is definitely yes. Although both domains carry exactly the same information, it may be more easy to access this information in one

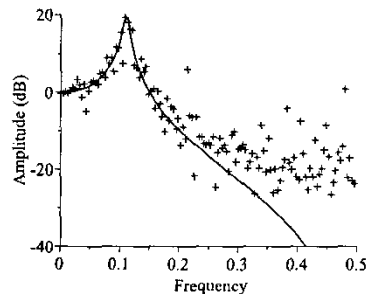


FIG. 1. Comparison of the true FRF  $G_0$  (—) with the estimated FRF  $\hat{G}$  (+)

domain than in the other because the same information is represented differently.

When discussing the differences between time- and frequency domain methods, a clear distinction should be made between the aspects that are intrinsically due to the frequency domain formulation, and on the other hand the additional signal processing possibilities that are opened by using periodic excitations. The latter might also be useful for time domain identification methods.

The practical aspects that take advantage of the frequency domain formulation are: arbitrary selection of the active frequencies where the model is matched to the measurements; continuous-time modelling; and identification of unstable models. By including also periodic excitations, we will be able to address in addition: the use of nonparametric noise models; separation of plant and noise model estimation; errors-in-variables identification and identification under feedback; separation of nonlinear distortions and (process) noise. These aspects are discussed in Section IV and V. A comprehensive discussion of other aspects can be found in (Pintelon and Schoukens, 2001; Ljung, 2004).

In Section VI, an extensive case study on the closed loop identification of a compact disc servo-system is presented. A frequency domain approach using periodic excitations is made. Many of the aspects mentioned before are illustrated.

### II. SETUP

The discussion in this paper is completely focused on single-input-single-output linear systems (SISO), but the reader should be aware that many results can be directly extended and generalized to multiple-input-multiple-output (MIMO) systems, and even a nonlinear behaviour can be included in the framework (Schoukens *et al.*, 2003).

Consider the discrete time system

$$y(t) = G_0(q)u_0(t) + H_0(q)e(t) = y_0(t) + v(t), \quad (1)$$

with  $t: -\infty \rightarrow \infty$ , and  $x(t-1) = q^{-1}x(t)$ . The aim of system identification is to extract the best model  $G(q, \theta)$  for the plant  $G(q)$ , and at times the disturbing noise power spectrum  $|H(q, \theta)|^2$ .

### III. TRANSIENTS: THE KEY TO THE EQUIVALENCE OF TIME AND FREQUENCY DOMAIN

In practice the identification should be done from a finite set of measurements

$$u_0(t), y(t), t = 0, 1, \dots, N-1. \quad (2)$$

The description (1) should be extended to include the impact of reducing the observation window from

$t : -\infty \rightarrow \infty$  to  $t = 0, \dots, N-1$ . This is illustrated in FIG. 2. The records are split in three parts: the observation window, the preceding and following unobserved signals. Two effects can be seen:

i) The past excitation (before the start of the observation  $t = 0$ ) contributes to the output in the observation window: a tail is added to the observed output (FIG. 2.a). These effects are well known in the time domain, a transient term  $T_G(t)$  has to be added to describe the contributions of the initial conditions to the output.

ii) When the data are processed in the frequency domain, it is implicitly assumed that the observed signals are periodically repeated. At that moment not only the tail (a) is added to the output, also the tail (b) will be missing. Although this looks more complicated than the previous situation it leads eventually to expressions that are completely equivalent to the time domain description. Both extended models are given below.

#### A. Extended time domain description

The reduction from  $t : -\infty \rightarrow \infty$  to  $t = 0, \dots, N-1$  adds initial conditions effects on the output of the dynamic systems (plant and noise filter). These are described by the plant and the noise filter transients  $T_G(t)$ ,  $T_H(t)$ . Both decay exponentially to zero.

$$y(t) = G_0(q)u_0(t) + H_0(q)e(t) + T_G(t) + T_H(t), \quad t \geq 0. \quad (3)$$

#### B. Extended frequency domain description

The finite data records  $\{u_0(t), y(t) : t = 0, \dots, N-1\}$  are transferred to the frequency domain using the discrete Fourier transform (DFT):

$$X(k) = \frac{1}{\sqrt{N}} \sum_{t=0}^{N-1} x(t) e^{-j\frac{2\pi}{N}tk}, \quad k = 0, 1, \dots, N-1 \quad (4)$$

with  $x = u, y, e$ , and  $X = U, Y, E$ . Although the spectra  $U_0, Y_0$  are affected by leakage, their relation remains remarkably simple: it is again sufficient to add a transient term to the system equations, completely similar to what is

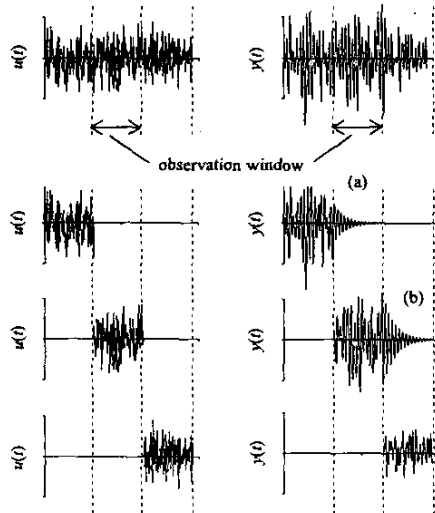


FIG. 2. : Illustration of the effect of the finite observation window.

done in the time domain (Pintelon *et al.*, 1997; Pintelon and Schoukens, 2001). This term describes the impact of the tails (a) and (b) on the input-output relation.

$$Y_0(k) = G_0(z_k^{-1})U_0(k) + T_G(k). \quad (5)$$

The relation between  $U_0, E$  and  $Y$  is:

$$Y(k) = G_0(z_k^{-1})U_0(k) + H_0(z_k^{-1})E(k) + T_G(k) + T_H(k),$$

$$\text{with } z_k = e^{j2\pi k/N}. \quad (1)$$

The reader should be aware that this expression is valid for arbitrary signals, no periodic excitation is required.

Loosely spoken, the impact of the transients disappears at a rate of  $N^{-1/2}$  or faster. In practice the noise transient  $T_H$  is always omitted. For simplicity we do the same in this paper.

#### C. Equivalence between time- and frequency domain

During the identification step, parametric plant- and noise models are identified by minimizing the squared prediction errors. This can be done in the time- or in the frequency domain (Ljung, 1999; Soderstrom, and Stoica, 1989):

$$V_{PE}(\theta, Z) = \sum_{t=0}^{N-1} |H^{-1}(q, \theta)(y(t) - G(q, \theta)u_0(t) - T_G(q, \theta))|^2$$

$$= \sum_{k=0}^{N-1} \frac{|Y(k) - G(z_k^{-1}, \theta)U_0(k) - T_G(z_k^{-1}, \theta)|^2}{|H(z_k^{-1}, \theta)|^2}$$

( $Z$  stands for the data). (6)

Both expressions result in exactly the same value for the cost function, and this for arbitrary excitations. This establishes the full equivalence between the time- and frequency domain formulation of the prediction error framework.

Remark: The transfer function model and the transient model have very similar expressions:

$$G(z_k^{-1}, \theta) = \frac{\sum_{n=0}^{n_b} b_n z^{-n}}{\sum_{n=0}^{n_a} a_n z^{-n}} T_{G(z_k^{-1}, \theta)} = \frac{\sum_{n=0}^{\max(n_a, n_b)} i_n z^{-n}}{\sum_{n=0}^{n_a} a_n z^{-n}} \quad (7)$$

Hence the inclusion of the transient term does not increase the complexity of the cost function because both rational forms have the same denominator.

#### D. Differences?

Although we established a full equivalence between the time- and frequency domain formulation, there are some remarkable differences in the practical use of these expressions.

1) Unstable plant models: If an unstable plant model is identified, the time domain calculations are tedious and often impossible because the calculation noise explodes. From Forsell and Ljung (2000) it is known that the predictor should be stable  $H^{-1}G$ . In the frequency domain, this problem is not a problem because only multiplications of the finite DFT-spectra are made, and the stability of the models

is not at the order, even not for the intermediate models during the iteration process (The zeros of  $H$  should be kept in the unite circle!).

2) It is very easy in the frequency domain to restrict the sum to a selected set of frequencies, for example the frequency band of interest; to those frequencies with a good signal-to-noise ratio; or to eliminate spurious components. Although this should not affect the prediction error result (it can be interpreted as a maximum likelihood estimator, and throwing away information does never improve the result), it has a strong impact on the calculation of initial estimates with sub optimal (linear) methods like ARX or subspace identification.

#### IV. PERIODIC SIGNALS: A FREE ACCESS TO THE NONPARAMETRIC NOISE MODEL

##### A. Introduction

The prediction error method can be considered as the solution of a weighted least squares problem:

$$V = \hat{v}^T C_v^{-1} \hat{v} \quad (8)$$

with  $\hat{v}^T = [\hat{v}(1) \dots \hat{v}(N)]$ ,  $\hat{v}(k) = y(k) - G(q, \theta_G)u_0(k)$ ,  $C_v$  the  $N \times N$  covariance matrix of  $v$ . The major problem is that  $C_v$  is a large dense matrix that should be inverted which is impractical. This is nicely circumvented in the prediction error method by whitening the residuals with a parametric noise model  $\epsilon(t) = H^{-1}(q, \theta)v(t)$ , leading to

$$V_{PE}(\theta, Z) = \epsilon^T \epsilon. \quad (9)$$

This is exactly the time domain form of  $V_{PE}(\theta, Z)$  in (5). In the frequency domain the matrix inversion does not come into play. The covariance matrix  $C_v$  of the frequency domain noise is asymptotically ( $N \rightarrow \infty$ ) a diagonal matrix:

$$C_v = \text{diag}[\sigma_Y^2(1) \dots \sigma_Y^2(N)], \quad (10)$$

with  $\sigma_Y^2(k) = |H(e^{j\omega_k})|^2$ . This gives an alternative frequency domain representation of the cost function:

$$V_{PE}(\theta, Z) = \sum_{k=0}^{N-1} \frac{|Y(k) - G(z_k^{-1}, \theta)U_0(k) - T_G(z_k^{-1}, \theta)|^2}{\sigma_Y^2(k)}. \quad (11)$$

The full details and the proof of the equivalence of (5) and (11) are given in Schoukens *et al.* (1999).

##### B. Taking advantage of periodic excitations

In the classical prediction error framework, the plant model  $G(q, \theta)$  and the noise model  $H(q, \theta)$  are identified simultaneously because this is the only possibility to separate the signal  $y_0(t)$  and the noise  $v(t)$ . However, if the excitation is periodical,  $u(t+T) = u(t)$ , it is possible to collect  $M$  successive periods, and to average the measurements over these repeated periods. This process is exemplified for the output measurement in FIG. 3.:

$$\hat{Y}(k) = \frac{1}{M} \sum_{l=1}^M Y^{[l]}(k),$$

$$\hat{\sigma}_Y^2(k) = \frac{1}{MM-1} \sum_{l=1}^M |Y^{[l]}(k) - \hat{Y}(k)|^2. \quad (12)$$

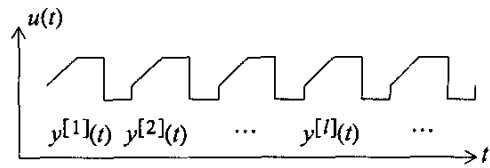


FIG. 3. Processing periodic excitations:  $y^{[l]}(t)$  is the  $l^{th}$  period.

The sample variance  $\hat{\sigma}_Y^2(k)$  is a nonparametric estimate of  $\sigma_Y^2(k)$ . Substituting it in the frequency domain expression of  $V_{PE}$  (11) gives:

$$V_{PE}(\theta, Z) = \sum_{k=0}^{N-1} \frac{|\hat{Y}(k) - G(z_k^{-1}, \theta)\hat{U}(k) - T_G(z_k^{-1}, \theta)|^2}{\hat{\sigma}_Y^2(k)}. \quad (13)$$

This results in a two step procedure: i) The nonparametric noise model  $\hat{\sigma}_Y^2(k) = \text{var}(\hat{Y}(k))$  is determined in the pre-processing step, ii) the plant model  $G(z_k^{-1}, \theta)$  is estimated in the 2nd step, keeping the noise model fixed.

##### C. Discussion

This approach has many advantages: i) It is no longer required to estimate plant and noise model simultaneously; ii) Even before starting the identification process, it is possible to verify the quality of the raw data as is illustrated in the example of Section VI; iii) The estimated noise model is no longer influenced by the plant model errors; iv) This method can be extended to the errors-in-variables problem. This includes identification in feedback as a special case.

The price to be paid for all these advantages is the restriction to periodic signals and the need for multiple periods to be measured, resulting in a frequency resolution loss. However, the required number of periods  $M$  can be small, for example  $M = 4$  is enough for consistency, and  $M = 6$  reduces the efficiency loss to less than 33% in variance (Schoukens *et al.*, 1997).

##### D. Extension: the errors-in-variables problem

In some applications, there is not only process noise on the output. Also the input measurements can be disturbed by noise, as is for example the case for identification in

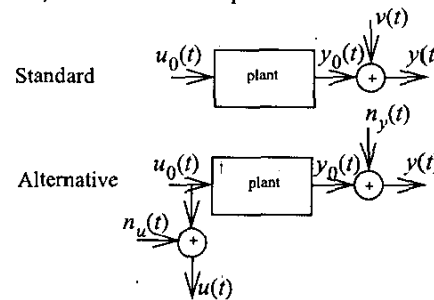


FIG. 4. : Standard and alternative noise assumption.

feedback. The nonparametric noise model is extended with the input noise variance  $\sigma_{U}^2(k)$  and the input-output covariance  $\hat{\sigma}_{YU}^2(k)$  ( $x$  denotes the complex conjugate):

$$\sigma_{YU}^2(k) = \frac{1}{MM-1} \sum_{l=1}^M (Y^{[l]}(k) - \hat{Y}(k))(U^{[l]}(k) - \hat{U}(k)) \quad (14)$$

The corresponding cost function to be minimized is the sample maximum likelihood (Pintelon and Schoukens, 2001):

$$V_{ML}(\theta, Z) = \sum_{k=1}^F \frac{|\hat{Y}(k) - G(\Omega_k, \theta) \hat{U}(k)|^2}{\sigma_Y^2(k) + \sigma_U^2(k) |G(\Omega_k, \theta)|^2 - 2 \text{Re}(\sigma_{YU}^2(k) \bar{G}(\Omega_k, \theta))} \quad (15)$$

The use of nonparametric noise models combined with identification in feedback is illustrated in Section VI.

## V. FREQUENCY DOMAIN IDENTIFICATION: A HIGHWAY TO CONTINUOUS TIME IDENTIFICATION

### A. Arbitrary excitation signals

In the last theory section of the paper, we combine the advantages of the time- and frequency domain identification approaches. A continuous-time modelling procedure is proposed using arbitrary excitations. The relation between the spectra of band limited measurements is the continuous-time model (see FIG. 5):

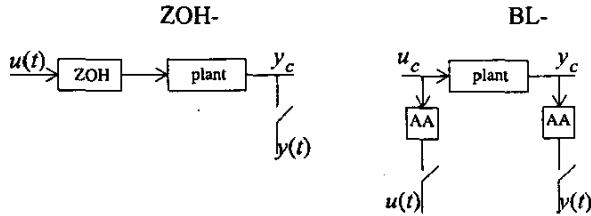


FIG. 5. : Ideal ZOH- and BL-setup. AA: an ideal anti-alias filter.

$$G(s, \theta) = \sum_{n=0}^{n_b} b_n s^n / \sum_{n=0}^{n_a} a_n s^n. \quad (16)$$

By combining this with a discrete time noise model, a mixed Box-Jenkins continuous time identification method is found that is based on the minimization of the cost function (Pintelon *et al.*, 2000):

$$V_{PE}(\theta, Z) = \sum_{k=0}^{N-1} \frac{|Y(k) - G(s, \theta)U(k) - T_{G(z_k^{-1}, \theta)}|^2}{|H(z_k^{-1}, \theta)|^2}. \quad (17)$$

The major advantages of this method compared to classical continuous time identification techniques are that: i) The need for approximate differentiation or integration is completely removed; ii) There is no need for huge oversampling rates, the full bandwidth can be used; iii) A noise model is included which increases the efficiency; iv) It is a logical extension of the well known Box-Jenkins identification method.

The major drawback compared with the discrete time Box-Jenkins method is the loss of consistency in feedback which is due to the mixture of a discrete- and continuous-time model.

### B. Periodic excitation signals

For periodic excitation signals the sample maximum likelihood method (15) can be used without any modification to identify a continuous-time model.

## VI. CASE STUDY: IDENTIFICATION OF A SERVO-SYSTEM IN CLOSED LOOP OPERATION

In this example we illustrate all the aspects that were discussed before:

- use of periodic signals
- extraction of a non parametric noise model
- use of a selected set of frequencies
- removal of large spurious components
- separation of the signals, the noise, and the nonlinear distortions
- identification of a continuous or discrete time model in feedback using the errors-in-variables frame work
- identification of an unstable model (due to nonlinear distortions);

### A. Experimental set-up

The open loop transfer function  $GC$  of the radial position servo-system of a CD player is identified. Figure 6 shows a simplified block diagram of the compact disc (CD)

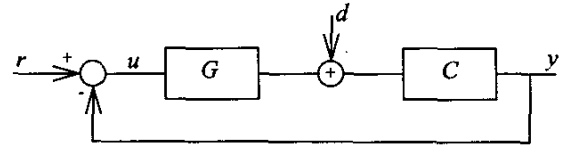


FIG. 6. Setup of the CD measurements.

player measurement setup. The block  $G$  stands for the cascade of a power amplifier, a lowpass filter, the actuator system and, finally, the optical position detection system. The block  $C$  stands for the parallel implementation of a lead-lag controller with some additional integrating action, that stabilizes the unstable actuator characteristics and takes care for the position control. In order to excite and to measure the open loop transfer function, two operational amplifiers have been inserted in between the lead-lag controller  $C$  and the power amplifier at the input of the process  $G$ .

### B. Need for closed loop identification

The actuator transfer function represents the dynamics of the arm moving over the compact disc, and is, in a first approximation, proportional to  $1/s^2$ . In practice, due to the friction, the double pole at the origin moves into the left half plane to a highly underdamped position. This explains why the characteristics of the position mechanism of a CD-player is very hard to measure in open loop.

### C. Use of the errors-in-variables framework

An external reference signal  $r$  is injected in the loop, the resulting signals  $u, y$  are measured (the input is not exactly known). Moreover, the loop is also disturbed by the process noise  $d$ , mainly induced by tracking irregularities due to potato shaped spirals; non eccentric spinning of the disc;

dirt, stains and scratches on the disc surface. The following relations exist between the Fourier spectra (assuming that they all exist):

$$\begin{aligned} U(j\omega) &= \frac{1}{1 + G(j\omega)C(j\omega)} R(j\omega) - \frac{C(j\omega)}{1 + G(j\omega)C(j\omega)} D(j\omega) \\ Y(j\omega) &= \frac{G(j\omega)C(j\omega)}{1 + G(j\omega)C(j\omega)} R(j\omega) + \frac{C(j\omega)}{1 + G(j\omega)C(j\omega)} D(j\omega) \end{aligned} \quad (18)$$

In the absence of disturbances, the open loop transfer function between  $u$  and  $y$  is  $G(j\omega)C(j\omega)$  and it is the aim of this section to provide a parametric model for it. A periodic reference signal  $r(t)$  will be applied, the contributions  $(C(j\omega)D(j\omega))/(1 + G(j\omega)C(j\omega))$  are considered as noise. Hence the input and output measurements are disturbed by mutually correlated noise which fits perfectly in the errors-in-variables approach.

#### D. Design of a periodic excitation, use of a well selected set of frequencies

For the sake of control, a 582.5 Hz sinusoidal wobble signal is internally injected in the feedback loop. It is measured at different points in the electronic circuit, and serves as an input signal for an automatic gain controller (AGC), to compensate, amongst other things, for the effect that the displacement of the arm is not perpendicular to the track over the whole disc, resulting in a variable gain of the process. The wobble signal complicates the measurement process significantly, since it is more than 20 dB above the normal signal levels in the loop. For this reason, we had to make a careful experiment design to eliminate its impact on the measurements.

As an external reference signal a multisine  $r(t) = \sum_{k=1}^F A_k \sin(2\pi f_0 l_k t + \varphi_k)$  with  $F = 305$ ,  $f_0 = 2.3842$  Hz,  $l_k = 1, 3, 9, 11, 17, 19, 25, 27, \dots$ , and  $A_k = \text{constant}$ , is used (Schoukens and Pintelon, 2001). The frequencies are selected to allow for the detection of nonlinear distortions at the non-excited frequencies. The multisine is generated with a clock frequency of  $10 \text{ MHz}/2^{10}$  and  $N = 4096$  points in one period.

#### E. Preprocessing: extraction of the signals and noise levels

In the first experiment, 256 K points are measured. The long record is broken in 16 blocks of 4 basic periods each ( $M = 16$ ). This is done in order to reduce the leakage effect of the wobble signal on the rest of the spectrum. The measurement window does not contain an integer number of periods of the wobble signal since its frequency is not synchronized to the measurement system (Figure 7). In this figure, it can be seen that the contribution of the reference signal is clearly above the disturbances level. Also the wobble signal (with its leakage) is clearly visible, its amplitude is more than 20 dB above the signals of interest.

Starting from the 16 repeated spectra,  $\hat{U}$ ,  $\hat{Y}$  are estimated, together with the (co-)variances  $\sigma_{\hat{U}}^2$ ,  $\sigma_{\hat{Y}}^2$ ,  $\sigma_{\hat{Y}\hat{U}}^2$  and shown in Figure 8. It turns out that there is an extremely high correlation ( $\sigma_{\hat{Y}\hat{U}}^2 / \sqrt{\sigma_{\hat{U}}^2 \sigma_{\hat{Y}}^2} \approx -1$ ) between the noise on  $U$  and  $Y$ . From (18), it is seen that this indicates that the process noise dominates completely the measurement noise

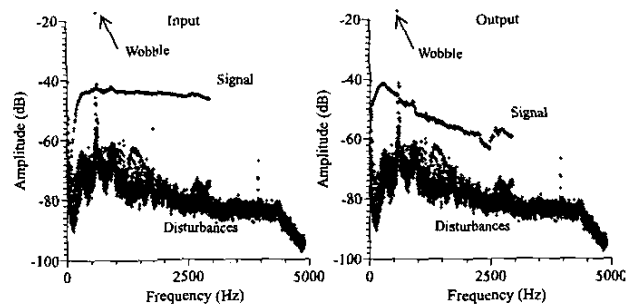


FIG. 7. Pilot test with a special odd multisine signal.

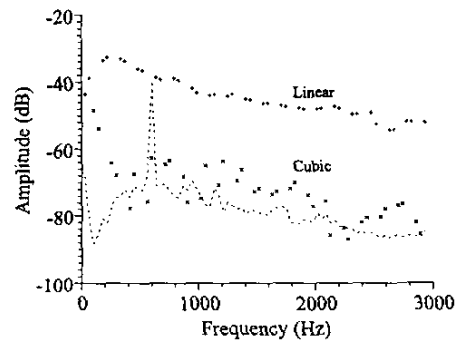


FIG. 9. nonlinearity test: power on the FRF measurement frequencies (linear), detected distortions after compensation for the linear feed through (cubic),  $-- \sigma_Y$ .

#### F. Quantifying the nonlinear distortions

Checking the non-excited odd frequencies in Figure 7 seems to indicate the presence of odd nonlinear distortions (Schoukens *et al.*, 1998; Pintelon and Schoukens, 2001; Schoukens *et al.* 2003), but they are almost completely hidden under the noise level of the test. Hence, a second experiment with a reduced set of frequencies: ( $f_0 = 19.07$  Hz with  $F = 39$ ) is made. This does not affect the relative level of the nonlinearities with respect to the linear contributions, but it increases the SNR (Pintelon and Schoukens, 2001). From the results in Figure 9 it is seen that the odd distortions are now well above the noise level of the test. Especially at the lower frequencies a very high distortion can be seen, indicating that the linearised models

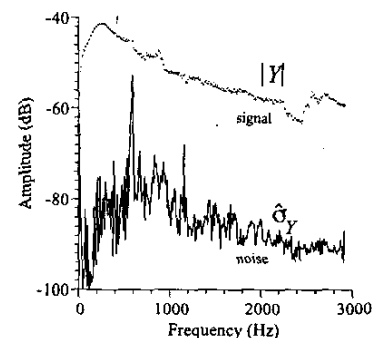


FIG. 8. SNR of the output measurements after processing the raw data.

will have poor value in this frequency band.

### G. Identification of a continuous or discrete time model

After these non-parametric tests, we have already a good idea about the limiting quality of the model. For the given input power, the nonlinearities are for sure less than 30 dB below the linear output. Next a linear model is identified that approximates the system as good as possible. A 24th order discrete-time or continuous time model ( $n_a = n_b = 24$ ) was identified (both give very similar results). The measured FRF is compared to the parametric model in Figure 10. As can be seen, a very good fit is obtained. The residuals are below the noise level. Only at the low frequencies, where the nonlinearities detected in the nonlinearity test are very large, the fit is poor. Because we knew in advance that in this band the data are of poor quality, the frequencies below 230 Hz were not considered during the fit. The cost function of the fit is 842.6, while a theoretical value of 256.5 is expected. This points to model errors. However, the auto-correlation of the residuals is white, therefore we can conclude that the best linear approximation is extracted. The remaining errors are due to the nonlinear behaviour of the process.

A stability analysis showed that two poles of the model were unstable ( $z = 1.021 \pm j0.00344$ ), but the corresponding closed loop model is stable and hence the model is valuable for a closed loop analysis. This instability is due to the fact that the system has 2 poles, almost equal to one (double integration in  $z$ -domain), that are very difficult to estimate due to the presence of the nonlinearities in this band.

## VII. CONCLUSIONS

In this paper the equivalencies and differences of time- and frequency domain identification are discussed. This discussion should not be mixed up with the use of periodic excitations.

The major conclusion is that there exist a full equivalence between both approaches from theoretic and information point of view. Transforming data from the time to the

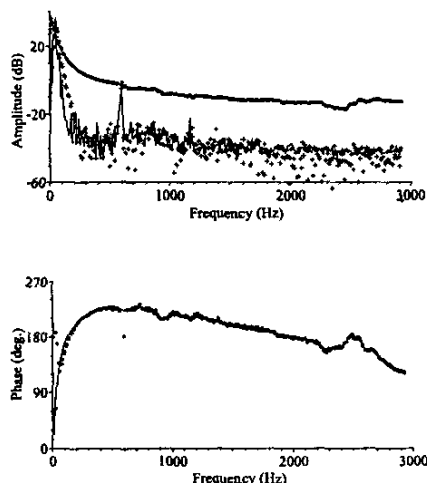


FIG. 10. : Comparison of the estimated transfer function (full line) with the measured FRF (dots). The residuals (+) are compared to the 95% noise level (thin full line).

frequency domain does neither create or delete information. Hence, what can be done in one domain can also be done in the other domain. However, in practice it might be easier to access the information in one of both domains. Arbitrary selection of active frequency bands, continuous time modelling, and identification of unstable models are typical examples.

It is also shown that the restriction to periodic inputs opens a number of practical possibilities and this for time- and frequency domain identification. It does not only allow to extract nonparametric noise models, it also simplifies significantly the identification under feedback conditions and gives access to a nonlinear distortion analysis.

## VIII. ACKNOWLEDGEMENT

This work was supported by the Flemish government (GOA-ILiNos), and the Belgian government as a part of the Belgian program on Interuniversity Poles of Attraction (IUAP V/22).

## REFERENCES

- [1] Forsell, U. and L. Ljung (2000). Identification of unstable systems using output error and Box-Jenkins model structures. *IEEE Transactions on Automatic Control*, 45, 131-147, 2000.
- [2] Ljung, L. (1987 and 1999). *System Identification: Theory for the User* (second edition). Prentice Hall, Upper Saddle River.
- [3] Ljung, L. (2004). State of the art in linear system identification: time and frequency domain methods. ACC 2004.
- [4] Pintelon, R., J. Schoukens and G. Vandersteen (1997). Frequency domain system identification using arbitrary signals. *IEEE Trans. on Automatic Control*, 42, 1717-1720.
- [5] Schoukens, J., R. Pintelon and Y. Rolain (1999). Study of Conditional ML estimators in time and frequency-domain system identification. *Automatica*, 35, 91-100.
- [6] Pintelon R., J. Schoukens, and Y. Rolain. *Box-Jenkins continuous-time modeling (2000)*. *Automatica*, 36, 983-991.
- [7] Pintelon R. and J. Schoukens (2001). *System Identification. A frequency domain approach*. IEEE-press, Piscataway.
- [8] Schoukens, J., R. Pintelon, G. Vandersteen and P. Guillaume (1997). Frequency-domain system identification using non-parametric noise models estimated from a small number of data sets. *Automatica*, 1073-1086.
- [9] Schoukens J., T. Dobrowiecki, and R. Pintelon (1998). Identification of linear systems in the presence of nonlinear distortions. A frequency domain approach. *IEEE Trans. Autom. Contr.*, Vol. 43, No.2, pp. 176-190.
- [10] Schoukens J., R. Pintelon, T. Dobrowiecki, and Y. Rolain (2003). Identification of linear systems with nonlinear distortions. *13th IFAC Symposium on System Identification*. Rotterdam, The Netherlands.
- [11] Soderstrom, T. and P. Stoica (1989). *System Identification*. Prentice-Hall, Englewood Cliffs